

Motion of Particles in Solar and Galactic Systems by Using Neumann Boundary Condition

Hossein Shenavar¹

Abstract A new equation of motion, which is derived previously by imposing Neumann boundary condition on cosmological perturbation equations (Shenavar 2016 a), is investigated. By studying the precession of perihelion, it is shown that the new equation of motion suggests a small, though detectable, correction in orbits of solar system objects. Then a system of particles is surveyed to have a better understanding of galactic structures. Also the general form of the force law is introduced by which the rotation curve and mass discrepancy of axisymmetric disks of stars are derived. In addition, it is suggested that the mass discrepancy as a function of centripetal acceleration becomes significant near a constant acceleration $2c_1a_0$ where c_1 is the Neumann constant and $a_0 = 6.59 \times 10^{-10} m/s^2$ is a fundamental acceleration. Furthermore, it is shown that a critical surface density equal to $\sigma_0 = a_0/G$, in which G is the Newton gravitational constant, has a significant role in rotation curve and mass discrepancy plots. Also, the specific form of NFW mass density profile at small radii, $\rho \propto 1/r$, is explained too. Finally, the present model will be tested by using a sample of 39 LSB galaxies for which we will show that the rotation curve fittings are generally acceptable. The derived mass to light ratios too are found within the plausible bound except for the galaxy F571-8.

Keywords Neumann Boundary Condition; Constant Acceleration in EoM; Precession of perihelion; Pioneer Anomaly; Galactic Rotation Curve; Galactic Mass Discrepancy.

Hossein Shenavar

Department of Physics, Ferdowsi University of Mashhad, Mashhad, Iran.
h.shenavar@gmail.com,
h.shenavar@mail.um.ac.ir

1 Introduction

The boundary condition of Einstein field equation has been debated since the beginning of the general theory of relativity. It has been shown that the Einstein-Hilbert action of general relativity is not well-posed in the sense that the boundary condition of the action is not compatible with the equations of field. See Krishnan & Raju (2016); Chakraborty (2016) and the references therein. The root of the problem is related to the fact that Einstein field contains second-order derivatives of the metric (Chakraborty 2016). However, one can overcome this obstacle by adding a boundary term to Einstein-Hilbert action to cancel the surface terms. In fact, as explained by Charap & Nelson (1983), there could be infinitely many boundary terms to do this. The most famous boundary term is the YGH boundary term (York 1972; Gibbons & Hawking 1977) which makes action invariant under diffeomorphism (Chakraborty 2016). In D dimension, we can write the YGH action which presumes Dirichlet boundary conditions, i.e. kills all the normal derivatives of the metric tensor on the surface, as

$$S = \frac{1}{2\kappa} \int_M d^D x \sqrt{g} (R - 2\Lambda) + \frac{1}{\kappa} \int_{\partial M} d^{D-1} y \sqrt{|h|} \epsilon K$$

in which $\kappa = 8\pi G$, R is the Ricci scalar, Λ is the cosmological constant, h is the induced metric on the boundary ∂M with the coordinates y , K is the extrinsic curvature of the boundary, g is the metric and $\epsilon = +1$ for timelike and -1 for spacelike boundaries. See Krishnan & Raju (2016); Chakraborty (2016) for proof. Also it has been shown by Krishnan & Raju (2016) that the action under Neumann boundary condition could be written as:

$$S = \frac{1}{2\kappa} \int_M d^D x \sqrt{g} (R - 2\Lambda) + \frac{D-4}{2\kappa} \int_{\partial M} d^{D-1} y \sqrt{|h|} \epsilon K$$

in which, surprisingly, the boundary term vanishes in four dimensions $D = 4$. Based on this action they have concluded that perhaps "*standard Einstein-Hilbert gravity in four dimensions, without boundary terms, has an interpretation as a Neumann problem*". This unique feature of imposition of Neumann BC on GR field equations suggests that this boundary condition might be more interesting than we have thought so far.

In a recent paper we imposed Neumann boundary condition to the equations of cosmological perturbation (Shenavar 2016 a). As a result of this new boundary condition, a modified Friedmann equation and a new lensing equation were found; where the latter was tested by a sample of ten strong lensing systems. In addition, we used the concept of geometrodynamics to modify the equation of motion of massive particles. We applied this equation to a sample containing 101 HSB and LSB galaxies and re-estimated the value of the Neumann constant which was found to be compatible with the prior evaluations from Friedmann and lensing equations. Moreover, by using a Newtonian approach we were able to derive the growth of structures in early universe and then we showed that the structures now grow more rapidly in matter dominated era.

In this work, I apply the new equation of motion of massive particles to solar and galactic systems. Also I compare the results with CDM model, Milgrom's modified Newtonian dynamics and Mannheim's fourth order conformal gravity. The CDM model tries to solve the apparent discrepancies between the dynamics of galactic - and also extra galactic - systems and their observed masses by assuming a dark halo around these systems (Sanders 2010; Navarro et al. 1996, 1997). Variety of obstacles like the so-called rotation curves of galaxies (Bottema et al. 2002; de Blok et al. 2008), the stability of galactic systems through numerical simulations (Ostriker & Peebles 1973; Mihos et al. 1997) and structure formation are solved by this assumption.

On the other hand, to solve the mentioned discrepancies, Milgrom (1983a,b,c) considered the possibility that the inertia term of Newton's second law is not proportional to the acceleration of the object, but rather is a more general function of it as $m\mu(\frac{a}{a_0})a = F$, in which a is the acceleration, a_0 is a constant acceleration, F is the force and the function μ - known as the interpolating function- plays a significant role at small accelerations (for example in galactic scales). Modified Newtonian dynamics (MOND) can perfectly explain asymptotic flatness of rotation curves (Bottema et al. 2002; Sanders 1996; Sanders & Verheijen 1998; Sanders & Noordermeer 2007). Also it is shown that the zero-point of the baryonic Tully-Fisher relation is of the order of Ga_0 which simply could be derived from

MOND equation of motion. The same is true for the zero-point of the Faber-Jackson relation in isothermal systems like elliptical galaxies (Milgrom 1984). There is also another quantity, $\sigma_0 = a_0/G$, which plays a significant role in galactic scales. Disks with mean surface density less than σ_0 have added stability (Milgrom 1989). In addition, σ_0 defines a transition central surface density and $\sigma_0/2\pi$ is very close to the central surface density of dark halos (Milgrom 2009). Moreover, this model simply explains that features in the rotation curve should follow the baryonic distribution; so the Renzo's rule which states that "For any feature in the luminosity profile there is a corresponding feature in the rotation curve" (Sancisi 2004; McGaugh 2004). Also, through this model, it seems that mass discrepancy is related to acceleration in units of a_0 (McGaugh 2004; McGaugh et al. 2016). The main point is that, after so many data fittings of experts working on MOND model, the role of a constant acceleration, a_0 , in galactic scales seems irrefutable now (Famaey & McGaugh 2012).

Another proposal to solve the dark matter problem is the fourth-order conformal theory of gravity (Mannheim & Kazanas 1989; Mannheim 1992, 1993, 1995), which is related to the present model because this theory too, predicts a constant acceleration. The field equation of this theory is derived from the action $I_w = -\alpha \int d^4x \sqrt{-g} C_{\lambda\mu\nu\kappa} C^{\lambda\mu\nu\kappa}$ where $C_{\lambda\mu\nu\kappa}$ is the conformal Weyl tensor and α is a purely dimensionless coefficient. This action leads to a fourth-order field equation which has an exact vacuum solution of the form $ds^2 = B(r)dt^2 - \frac{dr^2}{B(r)} - r^2d\Omega$ in which $B(r) = 1 - \frac{a}{r} + b + cr + \lambda r^2$. As it is clear, the fourth term on the rhs of $B(r)$ establishes a constant acceleration which plays a critical role in this theory. It has been shown that by using this added linear potential, one could capture the general trend of the rotation curve data to a good degree without needing any dark matter. In addition, obtained mass to light ratios, M/L , are close to the values of the local solar neighborhood (Mannheim & O'Brien 2012; O'Brien & Mannheim 2012). Conformal gravity claims that mass discrepancy in galactic scales is due to a global cosmological effect on local galactic motions. The cosmological constant problem too could be suppressed if we include the amount by which it gravitates (Mannheim 2006).

In the present work, I start by surveying the motion of a single particle subjected to the new equation of motion $a = g - 2c_1 cH(t)$ derived in Shenavar (2016 a). In this equation, a is the acceleration, g is the gravitational field, $H(t) = \dot{R}(t)/R(t)$ is the Hubble parameter, c is the speed of light and c_1 is the Neumann constant. We also use $a_0 = cH(t)$ to clarify the similarities with

MOND dynamics, though, the values are not quite the same. I will also study the effects of the new term $2c_1cH(t)$ in the scales of the solar system and I derive the precession of perihelion for some planets and dwarf planets. In the third section, the mentioned equation is applied to a system of particles and most importantly a modified force and potential is derived which is used in the next section to find the rotation curve of a disk galaxy. In the fifth section we study the functional dependence of mass discrepancy on radius, acceleration and gravitational field. Also we will argue that the present model can justify the radial dependence of NFW mass profile of dark halos and its constant surface density. Eventually, we use a data sample, that includes 39 LSB galaxies, to test the predictions of our model and then conclude our discussion with some final remarks.

2 The Motion of a Single Particle

We first consider the motion of a particle m in a gravitational field. As we discussed before, the modified equation of motion of this particle in a centrally directed gravitational field is as follows (Shenavar 2016 a):

$$\frac{d^2\vec{r}}{dt^2} + 2c_1a_0\hat{e}_r = g(r)\hat{e}_r \quad (1)$$

where $\vec{r} = r\hat{e}$ is the position of the particle, $a_0 = cH_0$ is a constant acceleration, also observed in Milgrom (1983a,b,c) modified dynamics with a different value, and $g(r)$ is the Newtonian field of gravity. Here we can put the new term $2c_1a_0\hat{e}_r$ on the lhs of the equation of motion and treat it as a modification to dynamics or, when we transfer $2c_1a_0\hat{e}_r$ to the rhs of Eq. (1), we can think of this term as a new force. These two approaches will eventually lead to the same results. For example, it is possible to show that both of these two scenarios result in the following conservation of energy E :

$$1/2m\vec{v}^2 + 2mc_1a_0r + V(\vec{r}) = E \quad (2)$$

where $V(\vec{r}) = -\int_{\vec{r}_0}^{\vec{r}} m\vec{d}x \cdot \vec{g}(\vec{x})$ is the gravitational potential energy. To prove this, one may consider $\vec{F} = m(g(\vec{r}) - 2c_1a_0)\hat{e}_r$ as a new force and use the definition of work done against this force in moving a particle from an initial place \vec{r}_0 to a final place \vec{r} :

$$W(\vec{r}) = \int_{\vec{r}_0}^{\vec{r}} \vec{d}x \cdot \vec{F} \quad (3)$$

Then it is possible to derive the conservation of energy (2) because the acting force is conservative. Another

way to obtain the conservation of energy is to directly integrate Eq. (1) to derive conservation of energy Eq. (2). As we mentioned, these two approaches are equivalent; however, we prefer to use the concepts of force and potential because the central force problem, which we need here, could be found in any standard textbook of theoretical mechanics and so it is customary to follow this approach.

From Eq. (1) one can prove that $\frac{d}{dt}(\vec{r} \times \frac{d\vec{r}}{dt}) = 0$ which is expected because the model is spherically symmetric. Therefore, similar to any spherically symmetric model, the particle here moves in a plane which is known as the orbital plane. Now, by using plane polar coordinate (r, ψ) and define the Lagrangian of the motion as follows:

$$\mathcal{L} = \frac{1}{2}m(\dot{r}^2 + (r\dot{\psi})^2) - \Phi, \quad (4)$$

in which $\Phi = \Phi_N + 2mc_1a_0r$ is the total potential and Φ_N is the Newtonian potential energy, it is possible to derive the equations of motion from Euler-Lagrange equation (Goldstein et al. 2002):

$$m\ddot{r} - mr\dot{\psi}^2 + \frac{d\Phi}{dr} = 0 \quad (5)$$

$$\frac{d}{dt}(mr^2\dot{\psi}) = 0 \quad (6)$$

The second equation shows that the quantity $l = mr^2\dot{\psi}$ is another constant of the motion which is known as the angular momentum. Another proof of the conservation of angular momentum $\vec{l} = m\vec{r} \times \vec{v}$ could be obtained by considering its rate $d\vec{l}/dt$, and using these facts that the external torques are negligible and we deal with a central force here.

The radial equation of motion (5) will contain only r and its derivatives if we replace ψ by l/mr^2 . Therefore, this equation will be equivalent to the equation of a one dimensional motion in which a particle is subjected to an effective potential of:

$$\Psi = \Phi_N + 2c_1ma_0r + \frac{l^2}{2mr^2} \quad (7)$$

where the third term on the rhs is due to the familiar centrifugal force. From Eq. (2) one can rewrite the conservation of energy as:

$$E = \Psi + \frac{1}{2}m\dot{r}^2 \quad (8)$$

Now we will study this one dimensional model for the specific case of an attractive inverse-square law of force, i.e. the Kepler problem $\Phi_N = -\frac{k}{r}$ where a positive

k describes a force toward the center. First consider the escape velocity of a particle which is defined as the minimum velocity required to escape from the gravitational field. According to the discussion that we had before (Shenavar 2016 a), if the particle reaches the radius $R_0 \approx \frac{2c_1 a_0}{\Lambda} \approx 100 Mpc$, in which Λ is the cosmological constant, then it is free. The reason is that in this radius the repulsive force due to cosmological constant, $F_1 \approx m\Lambda r$, overcomes the total attractive force $F = m(g(r) - 2c_1 a_0)$. Although for most physical cases, one could neglect $g(r)$ at a distance like R_0 because $g(R_0) \ll 2c_1 a_0$. Thus from Eq. (8) the escape velocity is approximately $v_0^2 \approx 2c_1 a_0 R_0$ and every particle with an energy larger than v_0^2 could come from infinity, strike the repulsive centrifugal barrier, be repelled and then travel back to infinity. These are very energetic particles. On the other hand all particles with smaller velocities than v_0 are bounded to the central object. For example consider a particle with energy E_1 in Fig. 1. For this particle there are two turning points, r_1 and r_2 , also known as "apsidal distances" (Goldstein et al. 2002). According to Bertrand's theorem, which states that the only central forces that result in closed orbits are the inverse-square law and Hooke's law (Goldstein et al. 2002), orbits of the present model are not closed because we have an added constant force too. However, if energy of the particle coincides with the minimum of the effective potential then $r_1 = r_2$ and the orbit is a circle and thus closed.

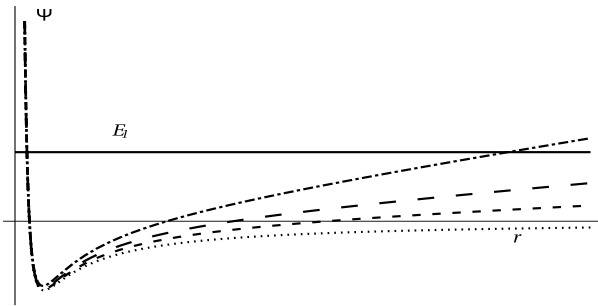


Fig. 1 General outline of the effective potential Ψ as a function of radius r . A particle with total energy E_1 would have two turning points.

Another important feature of Eq. (1) is that for this new equation of motion the famous Laplace-Runge-Lens (LRL) vector is not a constant of the motion anymore. We will show this below, however we should mention that in the Kepler problem beside four independent constants of the motion, i.e. the three elements of angular momentum vector and the energy, LRL vector is another constant which always points in the same direction known as the line of apsides (Goldstein et al.

2002). In the present model though, the cross product of Eq. (1) with the constant angular momentum \vec{l} results in (after a little manipulation):

$$\frac{d}{dt}(\vec{p} \times \vec{l} - mk \frac{\vec{r}}{r}) = 2c_1 m^2 a_0 (r \dot{\vec{r}} - \dot{r} \vec{r}) \quad (9)$$

where \vec{p} is momentum of the particle, k depends on the mass of the particle and the mass of the source of the gravity while $\vec{A} = \vec{p} \times \vec{l} - mk \frac{\vec{r}}{r}$ is the LRL vector. Although \vec{A} is not a constant anymore, which means that the line of apsides changes direction, a natural question is whether there is any other constant of the motion. The answer, which is no, is connected to the nonclosed nature of the orbits. See Goldstein et al. (2002) page 105. As we discussed before, due to Bertrand's theorem, the orbitals of Eq. (1) are nonclosed; therefore, as ψ goes around the particle never retraces its footsteps on any previous orbit. Thus r is an infinite-valued function of ψ and so the additional conserved quantity of the motion should involve an infinite-valued function of ψ too. So there is no more simple-defined constant of the motion.

Before we turn to the problem of a system of particles, which is needed to describe galactic phenomena, we consider the perturbation effect of a_0 -term in Eq. (1) on the outer objects of the solar system. To do so, we use $\eta = 2c_1 a_0 / g_N$ as a measure of the strength of the new term in (1) relative to the Newtonian gravitational field g_N . Using this parameter, near the surface of the Sun we have $\eta \approx 10^{-14}$, the Earth $\eta \approx 10^{-9}$, Neptune $\eta \approx 10^{-6}$ and Eris (one of the last dwarf planets) $\eta \approx 10^{-5}$. Therefore the new term is very small compared to the Newtonian gravity term in the solar system.

[t]

Although the expected effects are very small, it is still possible to find some clues of the new term in the scale of solar system. For example, one can use canonical perturbation theory to evaluate precession rate averaged over a period of unperturbed orbit τ as (Goldstein et al. 2002):

$$\bar{\omega} = \frac{\partial \overline{\Delta H}}{\partial l} \quad (10)$$

where $\Delta H = 2c_1 m a_0 r$ is the perturbation Hamiltonian and

$$\overline{\Delta H} = \frac{2c_1 m a_0}{\tau} \int_0^\tau r dt \quad (11)$$

is the time average of the perturbation. Then by using the conservation of angular momentum, i.e. $l dt = m r^2 d\psi$, the last integral converts to:

$$\overline{\Delta H} = \frac{2c_1 m^2 a_0}{l \tau} \left(\frac{l^2}{mk}\right)^3 \int_0^{2\pi} \frac{d\psi}{[1 + e \cos(\psi - \psi')]^3} \quad (12)$$

Table 1 Derived precession of perihelion $\bar{\omega}$ for two planets and two dwarf planets in arc seconds per century $''/cy$. Data of semi major axis A in AU , eccentricity e , orbital period τ (year) are derived from NASA <http://nssdc.gsfc.nasa.gov/>.

Object	A (AU)	e	τ (y)	C	rev/cent	$\bar{\omega}_{GR}$ ($''/cy$)	$\bar{\omega}_{a_0}$ ($''/cy$)
URANUS	19.2	0.046	83.7	6.323	1.195	2.4×10^{-3}	21.128
NEPTUNE	30.05	0.011	163.7	6.286	0.611	7.8×10^{-4}	41.333
PLUTO	39.48	0.245	247.9	7.558	0.403	4.2×10^{-4}	50.052
ERIS	67.781	0.433	558	11.546	0.179	1.2×10^{-4}	74.843

Table 2 Derived precession of perihelion $\bar{\omega}$ for four inner planets and the asteroid Icarus in arc seconds per century $''/cy$. Data of semi major axis A in AU , eccentricity e , orbital period τ (year) are derived from NASA <http://nssdc.gsfc.nasa.gov/>. The observed values of perihelion precession are reported in [d’Inverno \(1998\)](#) page 198 except for Mars which is reported in [Ohanian & Ruffini \(2013\)](#). All results of $\bar{\omega}_{a_0}$ are within the accepted bounds of the data.

Object	A (AU)	e	τ (y)	C	$A/A_{Neptune}$	rev/cent	$\bar{\omega}_{obs}$ ($''/cy$)	$\bar{\omega}_{GR}$ ($''/cy$)	$\bar{\omega}_{a_0}$ ($''/cy$)
MERCURY	0.387	0.205	0.241	7.157	0.0129	414.9	43.1 ± 0.5	42.96	0.06
VENUS	0.723	0.007	0.615	6.284	0.0241	162.6	8.4 ± 4.8	8.63	0.15
EARTH	1.	0.017	1	6.288	0.0333	100	5.0 ± 1.2	3.84	0.25
MARS	1.52	0.094	1.88	6.453	0.0506	53.2	$1.32 \pm ?$	1.35	0.47
ICARUS	1.078	0.837	1.12	149.913	0.0359	89.3	9.8 ± 0.8	10.04	0.66

in which e is the eccentricity and ψ' is one of the turning angles of the orbit. It is also possible to evaluate the precession rate from the average rate of LRL vector $(1/|\vec{A}|)d\vec{A}/dt$; though we prefer to use the standard method of ([Goldstein et al. 2002](#)). Anyway, one can calculate the integral in the last equation for any given eccentricity e ; the result, say C , is most likely of the order of 10. See [Table 1](#) and [2](#) for the magnitude of C for some important objects of the solar system. Then, from [Eq. \(10\)](#) the averaged precession rate is as follows:

$$\bar{\omega}_{a_0} = \frac{8c_1 C}{\tau} \frac{A^2 a_0}{GM} (1 - e^2)^2 \quad (13)$$

where M is the mass of the Sun and we have used the relation $l^2 = mkA(1 - e^2)$ which is correct for an unperturbed orbit with a semimajor axis A ([Goldstein et al. 2002](#)). In fact, [Sultana et al. \(2012\)](#) have found the perihelion shift of a test particle in fourth-order conformal gravity by tracking timelike geodesics which is compatible with the present result. Of course, one expects this agreement because both models are mainly based on linear potential terms.

We should point out that [Eq. \(13\)](#) is independent of the mass of the planet and so it represents a shear geometrical effect. The same is true about the conventional precession equation of GR. However, it should be mentioned that we expect a geometrical precession rate in both models, because the underlying field equation, i.e. Einstein’s field equations, are geometrical; though, here we have used a different boundary condition as discussed in the Introduction. In addition, from

[Eq. \(13\)](#) it is clear that orbits with larger semimajor axis will show larger precession rate. Therefore this effect should be more apparent in outer parts of the solar system. See [Table 1](#) for derived perihelion precession per century of two planets -Uranus and Neptune- and two dwarf planets - Pluto and Eris. In this table we have assumed that $a_0 = 6.59 \times 10^{-10} m/s^2$.

As we know, general relativity predicts another correction to Newtonian motion that can be described by a potential proportional to $1/r^3$. This term comes from Schwarzschild solution of Einstein field equation in strong field limit around the Sun ([Ohanian & Ruffini 2013](#)). By using the same method as we applied here, one can evaluate precession rate averaged over a period for the GR case as $\bar{\omega}_{GR} = \frac{6\pi}{\tau(1-e^2)} \left(\frac{GM}{c^2 A} \right)$. See [Goldstein et al. \(2002\)](#) for full derivation. For the planet Mercury we have $\bar{\omega}_1 \approx 0.10''$ per revolution or $42.96''$ per century. [Table 2](#) demonstrates our model’s prediction about inner planets. In fact, to have a reliable model of precision rate of inner plants, we should include the effects of all planets on inner ones. Therefore, full revisiting of the potential theory of the solar system is needed. This development is beyond the scope of the present work; thus, here we model the solar system by a uniformly distributed sphere of mass to roughly evaluate the effects of planets. As we will show in [Appendix A](#) - after we surveyed systems of particles in the next section - the acceleration at radius r of a uniformly distributed sphere by radius R_{sphere} is proportional to $2c_1 a_0 \frac{r}{R_{sphere}}$. Approximating the radius of the solar system by the semimajor axis of Neptune

$R_{sphere} = A_{Neptune} = 30AU$, we estimate the effect of the other planets on the inner ones, by multiplying a factor of $r/A_{Neptune}$ to Eq. (13). Therefore, for example in the Earth and Mercury we put $2c_1a_0 \frac{1AU}{30AU}$ and $2c_1a_0 \frac{0.387AU}{30AU}$ respectively, instead of $2c_1a_0$ to obtain the precession rate.

The derived precession rate of inner planets are reported in Table 2. In the case of Mercury, we find $\bar{\omega}_{a_0} = 0.06''/cy$ (arc seconds per century) and $\bar{\omega}_{GR} = 42.96''/cy$ while the observed value -subtracting the major effect of the Newtonian effects of the other planets - is equal to $43.1 \pm 0.5''/cy$ which shows that $\bar{\omega}_{a_0}$ stays within the observational bound. The same is true about Venus and Earth and asteroid Icarus as you may see in Table 13. In the case of Mars, the observational precession rate with its uncertainty could not be found, though, by investigating the uncertainties of the other planets shows that it should be around ± 0.5 or more. Therefore, Mars too is within our model. It is important to emphasize that although the effect of the new term $2c_1a_0$ is small compared to the GR effect, and very tiny compared to the Newtonian theory, it is not negligible at all. A thorough study of $\bar{\omega}_{a_0}$ of inner planets and also asteroids could help to evaluate its reliability, though, the best objects to search about such possible effects are the outer planets and the dwarf planets.

Because for orbits with large eccentricities, the value of C grow rapidly, we expect larger precession rates. For example, for $e = 0.8$ and $e = 0.9$ we have $C = 106.65$ and $C = 561.01$ respectively. The asteroid Icarus for example, which we talked about in the last paragraph, has an eccentricity of $e = 0.837$ and so $C = 149.913$. High eccentricities are also common for comets. This could be a helpful clue in our future investigations. Consider, for now, the Halley's comet with eccentricity of $e = 0.967$ and semimajor axis of $17.94AU$. This comet makes a perfect case for the reason that it has a very high eccentricity and one can derive $C = 8589$ and $\bar{\omega}_{a_0} = 108.96''/cy$. Although it should be mentioned that the factor $(1 - e^2)^2$ is significant here too because it decreases the precession for large eccentricities. On the other hand, consider the comet Chiron with $A = 13.7AU$ and $e = 0.383$. Data are again from NASA. For this comet one can find $C = 10.02$ and $\bar{\omega}_{a_0} = 14.69''/cy$. Thus the precession rate in the orbit of Halley's comet should be larger by almost an order of magnitude than the precession rate in the orbit of Chiron. The question is whether this new term could explain some peculiar features of the motion of comets in the solar system. However, this issue is beyond the scope of our work because in the case of comets we have some close encounters with Jupiter and Saturn. Also the possibility of nongravitational

forces should be included too (Newburn & Yeomans 1982). The point here is that if Eq. (1) is supposed to be correct, one should be able to detect its effects at the scales of the solar system.

At the scales of the solar system, one can find some other independent evidence too. For example, tracking data of Pioneer 10 and 11 spacecraft have shown a systematic unmodeled acceleration about $(8.74 \pm 1.33) \times 10^{-10} m/s^2$ directed toward the Sun (Anderson et al. 1998, 2002a,b). If there is indeed such added acceleration as Eq. (1) at solar scale, it must have some effects on small objects of the this system too. In fact, Wallin et al. (2007) considered the idea of an added constant acceleration, selecting a well-observed sample of trans-Neptunian objects with orbits between 20 and 100 AU from the Sun, and placed tight bound on the magnitude of the constant acceleration. According to this research, the deviation from inverse square law of gravity should be about $8.7 \times 10^{-11} m/s^2$ to $1.6 \times 10^{-10} m/s^2$. This estimation supports the value of the added acceleration of the present model, i.e. $2c_1a_0 = 8.6 \times 10^{-11}$ though it is more close to the lower bound.

Even in larger scales of the solar system like the Oort cloud, Iorio (2012) has shown that a constant acceleration toward the Sun could make bound trajectories and these trajectories radically differ from those of the Newtonian theory. Therefore, we see that there are some clues that support the existence of a constant acceleration in the scale of solar system and therefore, it is now safe to test Eq. (1) in larger scales like galaxies and clusters of galaxies. To do so, we need to investigate the issue of a system of particles all interacting according to Eq. (1).

Before we discuss systems of particles, we should point out alternative models too have some predictions about precession rate in solar system. For instance, Gron & Soleng (1996) assumed a constant density of dark matter in solar system in hydrostatic equilibrium. Then, based on the uncertainties in the perihelion precession of the asteroid Icarus, which is about 8%, they have shown that the density of DM would be about $\rho_0 \leq 1.8 \times 10^{-16} g/cm^3$ which is about 7 orders of magnitude larger than average galactic mass density. Therefore, we should conclude that either the uncertainty in the data could not be attributed to DM or the current data of the perihelion precession do not put strict limits on the density of it.

Fourth-order conformal gravity, on the other hand, has succeeded in matching data and predictions in the case of perihelion precession. Sultana et al. (2012) have used data for perihelion shift observations and found constraints on the value of the fundamental constant of fourth-order gravity which coincides with that obtained by using galactic rotational curves.

3 Systems of Particles

In this section the mechanics of a system of particles will be studied. To do so, we need some new definitions. Suppose that \vec{F}_i^e is the external force on the i th particle, with mass m_i , and let $\vec{F}_{ij}^N = \frac{Gm_1m_2}{r_{ij}^2}\hat{e}_{ij}$ be the Newtonian force exerted on the i th particle by the j th particle (with r_{ij} being the distance between the two particles and unit vector \hat{e}_{ij} pointing from i to j) and finally $\vec{F}_{ij}^{a_0}$ be the term due to acceleration transformation. Clearly one has $F_{ii}^N = F_{ii}^{a_0} = 0$ and also $\vec{F}_{ij}^N = -\vec{F}_{ji}^N$. On the other hand, because $\vec{F}_{ij}^{a_0}$ is proportional to a constant acceleration we have:

$$\frac{F_{ij}^{a_0}}{F_{ji}^{a_0}} = \frac{m_i}{m_j} \quad (14)$$

Using these definitions, the equation of motion of the i th particle under the influence of external and internal forces is as follows:

$$m_i\ddot{\vec{r}}_i = \vec{F}_i^e + \sum_j (\vec{F}_{ij}^N + \vec{F}_{ij}^{a_0}) \quad (15)$$

while, if the last equation is summed for all other particles, it takes the form of:

$$\sum_i m_i\ddot{\vec{r}}_i = \sum_i \vec{F}_i^e + \sum_{ij} (\vec{F}_{ij}^N + \vec{F}_{ij}^{a_0}) \quad (16)$$

Now it is possible to introduce four useful quantities: the center of mass or weighted average of the radii vectors of particles $\vec{R} = 1/M \sum m_i\vec{r}_i$, total linear momentum of the particles $\vec{P} = \sum m_i \frac{d\vec{r}_i}{dt}$, summation of radii $\vec{Q} = \sum \vec{r}_i$ and summation of velocities $\vec{\Pi} = \sum \frac{d\vec{r}_i}{dt}$. We use these definitions to prove the following important theorem:

Theorem 1. *a) If the total external force is zero and \vec{F}^{a_0} is negligible, then the total linear momentum \vec{P} is conserved,*

b) If the total external force is zero and the Newtonian gravitational force \vec{F}^N is negligible, then the summation of velocity $\vec{\Pi}$ is conserved,

c) If the total external force is equal to zero, but neither Newtonian gravitational force nor the force due to constant acceleration \vec{F}^{a_0} are negligible, then neither \vec{P} nor $\vec{\Pi}$ are conserved.

Proof. Part a). Under the conditions of part (a) which refer to strong field limit, the rhs of (16) is equal to zero since the law of action and reaction states that each pair $\vec{F}_{ij}^N + \vec{F}_{ji}^N$ is zero. Thus the total linear momentum is conserved. Part b). In this case, which refers to weak field limit, it is easier to start from (1) and sum over all

particles. Then it follows:

$$\sum_i \ddot{\vec{r}}_i = \sum_i \frac{\vec{F}_i^e}{m_i} + \sum_{ij} \left(\frac{\vec{F}_{ij}^N}{m_i} + 2c_1a_0\hat{e}_{ij} \right) \quad (17)$$

For every two particles i and j , the last terms on the rhs of this equation $2c_1a_0\hat{e}_{ij}$ are equal and opposite and so cancel each other. Now, if the total external force \vec{F}^e is zero and the Newtonian gravitational force \vec{F}^N is negligible, then it is clear that the rhs of Eq. (17) is equal to zero and so $\vec{\Pi} = \sum \frac{d\vec{r}_i}{dt}$ is a constant of the motion. Part c). This case is clear from Eqs. (16) and (17) because the rhs of none of these equations would vanish if neither Newtonian gravitational force nor the force due to constant acceleration \vec{F}^{a_0} are negligible. However there is an important exception here: if all particles in a system have the same mass then both \vec{P} and $\vec{\Pi}$ are conserved. \square

As an example, let us consider the important case of a two-body system. Suppose that the total external force is negligible, then by adding equations of motions of these two particles, it is possible to find equation of motion of the center-of-mass:

$$M\ddot{\vec{X}} = 2c_1a_0\hat{e}_{12}(m_2 - m_1) \quad (18)$$

where $\vec{X} = 1/M(m_1\vec{x}_1 + m_2\vec{x}_2)$ is the center of mass position and $M = m_1 + m_2$ is the total mass of the system. Therefore the conservation of the total linear momentum of the system is violated unless the two particles have same masses $m_2 = m_1$ as we mentioned in the last paragraph. To derive the relative motion of m_2 and m_1 one should multiply the equation of motion of the former by m_2/M and the latter by m_1/M and then subtract to achieve:

$$\mu\ddot{\vec{x}} = \vec{F}_{12}^N + 4\mu c_1a_0\hat{e}_{12} \quad (19)$$

where $\vec{x} = \vec{x}_1 - \vec{x}_2$ is the relative position of the two objects and $\mu = \frac{m_1m_2}{M}$ is known as the reduced mass. As one expects, for the case that the two particles have the same mass m we obtain $m\ddot{\vec{x}} = \vec{F}_{12}^N + 2c_1ma_0\hat{e}_{12}$, which is exactly of the form of equation of motion of single particle under the influence of gravitational field \vec{F}_{12}^N and a constant acceleration.

To obtain the net force on a particle m_i at position \vec{x} from a system of particles, one should simply add the small contribution from each small particle. However, for a typical galaxy by about 10^{11} stars this method is not practicable. A good solution to this problem is to assume a smooth mass distribution which is proportional to the local star density $\rho(\vec{x}')$ at any point. According to Eq. (1), the tiny force exerted by a small element of mass (of a large mass distribution

) $dm' = \rho(\vec{x}')d^3x'$ positioned at \vec{x}' on a point particle m_i placed at \vec{x} is as follows:

$$\delta\vec{F}(\vec{x}) = Gm_i \frac{\vec{x}' - \vec{x}}{|\vec{x}' - \vec{x}|^3} \rho(\vec{x}')d^3x' + 2c_1a_0m_i \frac{\vec{x}' - \vec{x}}{|\vec{x}' - \vec{x}|} \quad (20)$$

Then the total force of the mentioned distribution on the point particle m_i can be deduced by summing these small contributions:

$$\vec{F}(\vec{x}) = m_i \left(G \int \frac{\vec{x}' - \vec{x}}{|\vec{x}' - \vec{x}|^3} \rho(\vec{x}')d^3x' + \frac{2c_1a_0}{M} \int \frac{\vec{x}' - \vec{x}}{|\vec{x}' - \vec{x}|} \rho(\vec{x}')d^3x' \right). \quad (21)$$

Here M is the total mass of the distribution. To obtain the second term on the rhs of (21) we used the fact that the acceleration due to the new term $2c_1a_0$ between m_i and the mass distribution should be the same. On the other hand, as Eq. (14) states, the ratio of the forces between these two parts is equal to the ratio of their masses and so we can obtain the last equation.

An interesting example to apply Eq. (21) to is the force between a spherical shell of matter, by mass M , and a particle of mass m inside or outside of the shell. For this problem, the first integral on the rhs of Eq. (21) refers to the famous shell theorems: *A uniform shell exerts no gravitational force on a particle inside the shell; the shell attracts an external particle as if all the mass of the shell were concentrated at its center.* For the second integral on the rhs of Eq. (21) it is straightforward to show that for an external particle the exerted force is $ma_0(1 - R^2/3r^2)$ while for an internal particle we find $2ma_0r/3R$. Here R represents the radius of the shell and r is the distance of the particle from shell's center. See appendix A for the derivation. Deriving the force for other symmetrical mass distributions - i.e. homogeneous sphere, an exponential sphere and an exponential disk - shows that for an internal particle the leading term of the force is always proportional to r/R . This is the reason that in the previous section we demanded to use $2c_1a_0\frac{r}{R}$ instead of $2c_1a_0$ in the case of inner planets like the earth. Furthermore, it is easy to check that the new force is always toward the center of the shell. In addition, from the symmetry, it is clear that there is no net force on a particle located at $r = 0$. We will use these results to have a better understanding of the solutions and their asymptotic behaviour.

As usual, we prefer to work with scalar quantities instead of vector ones. Having this in mind, we can define the potential $\Phi(\vec{x})$ of a distribution of matter by

$\Phi(\vec{x}) = \int \vec{F}(\vec{x}') \cdot d\vec{x}'$ and derive it as:

$$\Phi = -G \int \frac{\rho(\vec{x}')d^3x'}{|\vec{x}' - \vec{x}|} + \frac{2c_1a_0}{M} \int \rho(\vec{x}')d^3x'|\vec{x}' - \vec{x}| \quad (22)$$

where the first term is the Newtonian gravitational potential and the second one is the new potential due to the constant acceleration. This new term provides extra attracting force as we need in galactic scales.

It is clear that the Newtonian gravitational potential fulfills the Poisson equation; though the net potential Φ can not fulfill any second-order Poisson equation because of the presence of the new a_0 dependent potential $\Phi^{a_0} = \frac{2c_1a_0}{M} \int \rho(\vec{x}')d^3x'|\vec{x}' - \vec{x}|$. It is possible, however, to show that the new potential Φ satisfies a new fourth order Poisson equation:

$$\nabla^4\Phi = 4\pi G\nabla^2\rho_b - \frac{16c_1\pi a_0}{M}\rho_b. \quad (23)$$

in which ρ_b is the baryonic matter. It should be pointed out that higher-order Poisson equations are very common in beyond Einstein gravity. For example, in fourth-order conformal gravity or $F(R)$ gravities, we essentially deal with an action with higher-than-second order derivatives. Therefore, higher order Poisson equations emerge quite naturally without even considering systems of particles. In these theories one should deal with the problem of ghosts, i.e. negative norm states which break the unitarity. However, in the case of fourth-order gravity, it has been shown that the ghost states disappear from the eigenspectrum of the Hamiltonian (Mannheim 2006).

The situation in MOND is more complicated. In this model, a few modified Poisson equations have been proposed by using TeVeS or based on other related assumptions. See Famaey & McGaugh (2012) for a complete review. This model is basically nonlinear, though some linearized versions of its Poisson equations has been reported Famaey & McGaugh (2012). The nonlinearity poses serious problems in using this great model.

The Poisson equation of the present model, i.e. the last equation, is derived from a second-order action, i.e. Einstein-Hilbert action plus a boundary term. Thus it displays no ghost problem. Also it is genuinely linear and so more easy to use. We discuss this new Poisson equation in more detail in a forthcoming paper in which we survey the distribution of matter in galaxies (Shenavar 2016 b). Now we investigate the motion of particles in disk galaxies which is the main aim of the present work.

4 Rotation Curve of Spiral Galaxies

According to Newton's equation of motion, it is expected that the rotation velocity of particles orbiting around a massive object falls as $v^2 \sim \frac{1}{r}$ in which r is the radius of the particle. This behavior is known as the Keplerian fall-off of velocity and it is highly supported by the solar system data. However, at galactic scales such decline in the velocity has not been observed. In fact, because of the hydrogen gas which is distributed in galaxies to much further distances than their stars, we now have detailed knowledge about the rotation velocity of objects at galactic scales and it is now clear that there is a mass discrepancy at least for galaxies which have extended rotation curves beyond their optical radius. See Sanders (2010) for an excellent history.

According to Casertano & van Gorkom (1991), the rotation curve data of galaxies could be divided into three categories. First, the rotation curve of low luminosity dwarf galaxies, with maximum velocity smaller than 100 km/s, are typically rising. Second, those of intermediate to high luminosity galaxies, with $100 < v_{max} < 180$ km/s and $v_{max} > 180$ km/s respectively, are found to be flat. Third, the rotation curves of the very highest luminosity galaxies are generally declining from 15% for NGC2903 to 30% for NGC2683.

It is known that galaxies have very diverse mass distributions; however, for the sake of simplicity we consider the special case of disk galaxies here. The disk galaxies contain stars, gas and dust. There are also spiral structures with various shapes and lengths. We usually measure distribution of stars in a galactic disk by observing total stellar luminosity emitted by unit area of the disk, i.e the surface brightness. Observations suggest that the surface brightness of these galaxies is approximately an exponential function of radius: $I(r) = I \exp(-r/R_d)$; where R is the radius and R_d is the disk scale length. Scale lengths range from 1 kpc to more than 10 kpc; see (Binney & Tremaine 2008) page 26. While galactic disks are thin because mass density falls off much faster perpendicular to the equatorial plane than in the radial direction, it is believed that most spiral galaxies contain also a bulge, which is a centrally concentrated stellar system. Here we seek a thin disk rotation curve; the extension to a separable thick disk or a disk with a spherical bulge is straightforward.

If we suppose that, beside surface brightness of these galaxies, the disk surface mass density $\Sigma(R)$ is also exponential

$$\Sigma(R) = \Sigma_0 \exp(-r/R_d), \quad (24)$$

in which Σ_0 is the surface mass density at $r = 0$, then the total mass of the disk is $M = 2\pi\Sigma_0 R_d^2$. Following

an approach which Casertano (1983) has developed, by differentiating Eq. (22) with respect to r one could derive the circular velocity of the exponential disk:

$$v^2(r) = r \frac{\partial \Phi}{\partial r} = 4\pi\Sigma_0 G R_d y^2 [I_0(y)K_0(y) - I_1(y)K_1(y)] + 8c_1 a_0 R_d y^2 I_1(y)K_1(y) \quad (25)$$

in which I and K are modified Bessel functions and $y = r/2R_d$. Complete derivation of the last equation is presented in A. See also Mannheim (1993, 2006) for the same derivation related to another linear potential. One could also find the potential of a separable thick disk and a spherical bulge in the latter reference. If the structure is composed of two or more elements, for example a cold exponential disk plus some HI gas distribution with a specific profile, then one has to evaluate rotation curve for each element and add them up to derive the total rotation curve. For example, O'Brien & Mannheim (2012) have approximated the gas profile as single exponential disk with scale length equal to four times of those of the corresponding optical disk. This is a very successful approximation as fitted rotation curves clearly show (O'Brien & Mannheim 2012).

All departure from the standard Newtonian mechanics are embodied in the a_0 -dependent term of the Eq. (25). This term is competitive with the Newtonian one in outer parts of galaxies and clearly it predicts that the more luminous the galaxy, the less important a_0 term is; or the less hypothetical dark matter is needed. To see this, let us rewrite the last equation as a dimensionless form by dividing it by the maximum velocity of an

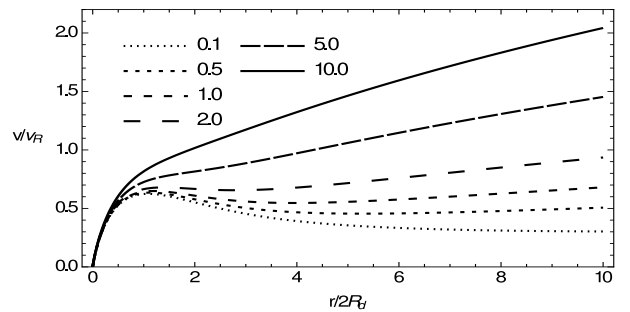


Fig. 2 Rotation velocity v in units of $v_R = \sqrt{GM/R_d}$ as a function of radius for different values of $\sigma_0/\Sigma_0 = 0.1, 0.5, 1.0, 2.0, 5.0, 10.0$. Low mass galaxies, i.e. galaxies with small Σ , show a clear rising rotation curve; those of intermediate- to high-mass galaxies have a relatively flat rotation curve, and those of the highest masses possess a Keplerian decline in their rotation curves to a large distance.

equivalent spherical distribution $v_R^2 = GM/R_d$:

$$\frac{v^2(r)}{GM/R_d} = 2y^2[I_0(y)K_0(y) - I_1(y)K_1(y)] + \frac{4c_1}{\pi} \frac{\sigma_0}{\Sigma_0} y^2 I_1(y)K_1(y) \quad (26)$$

where $\sigma_0 = a_0/G$ is a critical mass density. See Fig. 2 for a plot of this equation for various ratios of σ_0/Σ_0 . Regarding Eq. (26) it is evident that in galaxies with large surface mass density, i.e. large Σ_0 , the second term is less important while it would be dominant for galaxies with small surface density. In general, we see that the parameter σ_0/Σ_0 determines the general behavior of the rotation curve here.

Detailed rotation curve data for a sample of 39 galaxies will be presented in the last section; here, we seek theoretical clues of Eq. (1) for future investigations. Another important feature of this equation is that it suggests a constant acceleration, i.e. $2c_1a_0$, at large radii from the center of the disk. See Fig. 3 for a plot of the acceleration $a = v^2/r$ scaled by a_0 as a function of scaled radius $r/2R_d$ for different values of σ_0/Σ_0 . Outside of a disk, the acceleration as a function of radius could be approximated as $GM/r^2 + 2c_1a_0 - 3c_1a_0R_d^2/r^2$ which we have used asymptotic behavior of modified Bessel functions to derive the last result. See Appendix A for the formula for asymptotic behavior of Bessel functions. Therefore, it is clear that, although more massive galaxies reach a higher peak in their acceleration plot, the data of all galaxies should asymptotically converge to $2c_1a_0$ eventually. In our last paper (Shenavar 2016 a) we showed that for a sample of galaxies the accelerations of the last data points

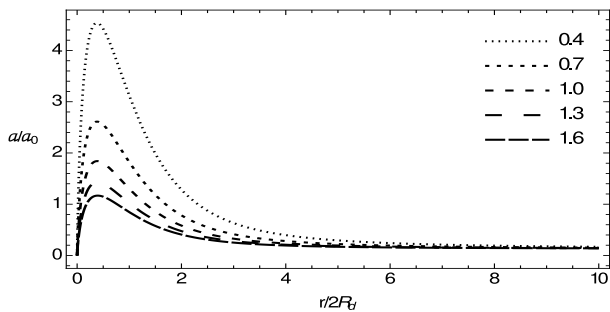


Fig. 3 Centripetal acceleration a in units of a_0 as a function of radius for different values of $\Sigma_0/\sigma_0 = 0.4, 0.7, 1.0, 1.3, 1.6$. Regardless of the mass, size and shape of galaxies the present model predicts that the centripetal acceleration should approach a constant value of $2c_1a_0$ while Newtonian theory of gravity predicts a decreasing centripetal acceleration as $1/r^2$. See Shenavar (2016 a) for a sample of galaxies which clearly suggests a constant acceleration at their last data points.

are close to this predicted value. This behavior is also strongly supported by Mannheim and O'Brien investigations (Mannheim & O'Brien 2012; O'Brien & Mannheim 2012). They have studied two different galaxy samples consisting of high surface brightness (HSB), low surface brightness (LSB) and dwarf galaxies with different masses, scales and rotation velocities. In the first sample they have considered 111 HSB, LSB and dwarf spiral galaxies. The second sample is consisted of 27 objects which most of them are dwarf galaxies. The data are such that the value of the quantity $(v^2/r)_{last} \approx 3 \times 10^{-11} m/s^2$ as measured at the last data point is near universal. This quantity is also very close to the constant acceleration of the conformal Weyl gravity which is numerically extracted from the data fitting of rotation curves (Mannheim 2006; Mannheim & O'Brien 2012; O'Brien & Mannheim 2012). In addition, MOND theory (Milgrom 1983a) and Moffat's metric skew-tensor theory (Brownstein & Moffat 2006), which have succeeded to explain galactic rotation curve, possess two similar universal parameters. For Mond theory one has $a_0 \approx 10^{-10} m/s^2$ and for MSTG theory $G_0M_0/r_0^2c^2 \approx 7.67 \times 10^{-29} cm^{-1}$ (Mannheim 2006; Brownstein & Moffat 2006). Even more support for a role of a universal acceleration could be found as we will discuss in the next section (McGaugh 2004; McGaugh et al. 2016). Therefore, it seems that the existence of a constant quantity should be regarded as an important empirical clue for galactic systems.

5 Mass Discrepancy

In any alternative theory of gravity it is important to find new quantities to illustrate differences between new theory, the Newtonian one and the CDM paradigm. One of these quantities is the mass discrepancy which is defined as the squared ratio of observed velocity v to the velocity that is attributable to Newtonian gravity of visible baryonic matter v_N , viz. $(\frac{v}{v_N})^2$ (McGaugh 2004; Famaey & McGaugh 2012). It has been shown that this quantity is well correlated with acceleration, and increases systematically with decreasing acceleration below the MOND parameter $1.2 \times 10^{-10} m/s^2$ (McGaugh 2004). In the present model it is easy to start from equation (26) and derive the mass discrepancy as a function of radius r , centripetal acceleration $a = \frac{v^2}{r}$ and Newtonian acceleration g_N as follows:

$$\left(\frac{v}{v_N}\right)^2 = 1 + 2c_1 \frac{\sigma_0}{\Sigma_0} \frac{I_1(y)K_1(y)}{I_0(y)K_0(y) - I_1(y)K_1(y)} \quad (27)$$

$$\left(\frac{v}{v_N}\right)^2 = \frac{a}{a - 4c_1a_0yI_1(y)K_1(y)} \quad (28)$$

$$\left(\frac{v}{v_N}\right)^2 = 1 + \frac{4c_1 a_0}{g_N} y I_1(y) K_1(y) \quad (29)$$

Let us investigate the implications of these three equations. Equation (27) predicts that in galaxies which surface mass densities are much smaller than σ_0 , mass discrepancy should exist everywhere. On the other hand, galaxies with a high surface density should show a larger mass discrepancy in their outer parts but not in their inner parts. Thus, mass discrepancy as a function of radius depends on the ratio σ_0/Σ_0 for all galaxies. See Fig. 4 for a plot of mass discrepancy as a function of radius for different values of σ_0/Σ_0 ratios. Also you may find data plots of mass discrepancy for various galaxies in [McGaugh \(2004\)](#). We should also point out that if there is a bulge at the center of the galaxy then one should expect a higher mass discrepancy at small radii; though, the mass discrepancy at large radii would not change significantly.

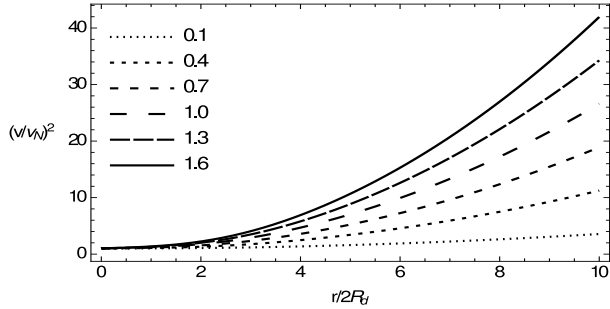


Fig. 4 Mass discrepancy as a function of radius for different values of $\Sigma_0/\sigma_0 = 0.1, 0.4, 0.7, 1.0, 1.3, 1.6$. For larger values of σ_0/Σ_0 the mass discrepancy is larger compared to the ones with smaller values of σ_0/Σ_0 .

[McGaugh \(2004\)](#) have shown that, regardless of the choice of stellar mass-to-light ratio, acceleration is the physical scale with which the mass discrepancy correlate best. See also [Famaey & McGaugh \(2012\)](#). On the one hand, equation (28) illustrates that for any galaxy when centripetal acceleration approaches to $2c_1 a_0$, we should see a large mass discrepancy. See figure 5. In addition, the special form of (28) seems generic for spiral galaxies; i.e. if equation (1) is correct, all of spiral galaxies should have the same relation between mass discrepancy and centripetal acceleration. This is an important point because the previous results, viz. Eqs. (25) and (27), seems to vary from galaxy to galaxy because they depend on the central surface density Σ_0 ; however equation (28) shows a unique character for all spiral galaxies. On the other hand, when centripetal acceleration is much larger than $2c_1 a_0$, for example at scales of the solar system, mass discrepancy is very

small. In these limits the mass discrepancy approaches to one. See the horizontal asymptote of Fig. 5. In addition, for any radius there is a vertical asymptote at $a \lesssim 2c_1 a_0$. Furthermore, from equation (29) we see a large mass discrepancy when g_N approaches to zero. However when g_N is much larger than $2c_1 a_0$, mass discrepancy is very small. To conclude, we should say that if equation (1) is ought to be the correct description of object's motion in galactic scales, equations (27), (28) and (29) should be applicable in any such scales, except around the centers of galaxies which we might need to use the strong field regime of the general theory of relativity.

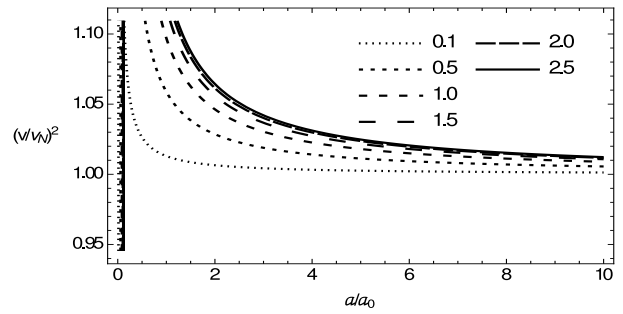


Fig. 5 Mass discrepancy $\left(\frac{v}{v_b}\right)^2$ as a function of centripetal acceleration a for different values of $y = r/R_d = 0.1, 0.5, 1.0, 1.5, 2.0, 2.5$. The horizontal line, $\left(\frac{v}{v_b}\right)^2 = 1$, indicates where there is no mass discrepancy; i.e. baryonic mass content is enough to explain the observed motion. It is expected, according to our model, that the mass discrepancy becomes important when $a < 4c_1 a_0$.

One last point: Comparing the squared of the observed velocity v and Newtonian velocity v_N , this time with their subtraction instead of their ratio, could make a useful result. From Eq. (25) it is easy to see that:

$$\frac{v^2 - v_N^2}{r} = 4c_1 a_0 y I_1(y) K_1(y) \quad (30)$$

where v and r are observable quantities and v_N could be derived ([McGaugh 2004](#)). Data plot of this last equation could directly disprove Eq. (1) if we find inconsistent results. On the other hand it is possible to define at any radius r , a dynamical mass which is attributable to the rotation velocity: $M_D = \frac{rv^2}{G}$. Then, starting from the last equation, one may obtain the difference between dynamical and Newtonian mass as follows: $M_D - M_N = 16c_1 \sigma_0 R_d^2 y^3 I_1(y) K_1(y)$; where M_N is the amount of Newtonian - or baryonic - mass inside radius r . Now we interpret the quantity $M_{DM} = M_D - M_N$ as the amount of "missing mass" or the dark matter mass, where clearly is related to the critical surface density $\sigma_0 = a_0/G$ but not to

the surface density Σ_0 of galaxies. Therefore the dark matter density distribution varies, very interestingly, as ($\rho_{DM} = \frac{dM_{DM}}{dV}$):

$$\rho_{DM} = \frac{c_1 \sigma_0}{2\pi R_d} \{I_1(y)K_1(y) + y(I_0(y)K_1(y) - I_1(y)K_0(y))\} \quad (31)$$

in which we have assumed a spherical shape for the dark halo, viz. $dV = 4\pi r^2 dr$. See Appendix A. The first interesting point is that according to this equation the density of the dark halo should vary proportional to the inverse of radius at small radii, i.e. $\rho_{DM} \approx (c_1 \sigma_0 / \pi)[r^{-1} + O(r^{-1})]$. We used Eqs. (A17) and (A18) in Appendix A to derive this asymptotic behavior. This behavior is the same as the behavior of the NFW mass profile for the galactic dark halos at small radii. Navarro, Frenk and White (NFW) used high-resolution N-body simulations to study density profiles of dark matter halos and found $\rho_{DM}^{NFW} = \frac{\rho_0}{(r/r_s)(1+(r/r_s))^2}$ (Navarro et al. 1996, 1997). They realized that all such profiles have the same shape, specially independent of the halo mass. Their specific mass profile changes gradually from $1/r$ to $1/r^3$ beyond a certain critical distance from the center known as the scale radius r_s . This special form of mass distribution reproduces galactic phenomena; however it provides an infinite mass for the dark matter halo (Binney & Tremaine 2008). The second important point about Eq. (31) is that it predicts a constant central surface density for dark halos $\frac{c_1 \sigma_0}{\pi}$, i.e. the central surface density should be independent of the total mass of galaxies. Interestingly, this is a famous observational result that was first noticed by Donato et al. (2009). See also Famaey & McGaugh (2012). Then Milgrom (2009) proved that MOND too predicts such central surface density for the dark halos as $a_{0,MOND}/(2\pi G) = 0.286 \text{ kg/m}^2$ which is close to our derived value of $\frac{c_1 \sigma_0}{\pi} = 0.204 \text{ kg/m}^2$. Therefore, we see that the present model explains the two important features of the NFW mass profile namely, i.e. its small radii behavior and its constant central surface density.

The point that the halo mass profile is dependent to the critical mass density σ_0 , nor the surface density of single galaxies Σ_0 , is a particularly interesting result. The reason is that we usually relate the observational quantities to the baryonic mass; e.g. rotation curves of galaxies and mass discrepancies as discussed here or TullyFisher relation which will be studied elsewhere (Shenavar 2016 b). Although, the mass profile that we predicted above, i.e. ρ_{DM} , is solely related to the halo and is independent of the baryonic mass. The fact that the present model can predict a property of a totally different paradigm, i.e. the DM hypothesis,

without even referring to the observational data seems quite notable.

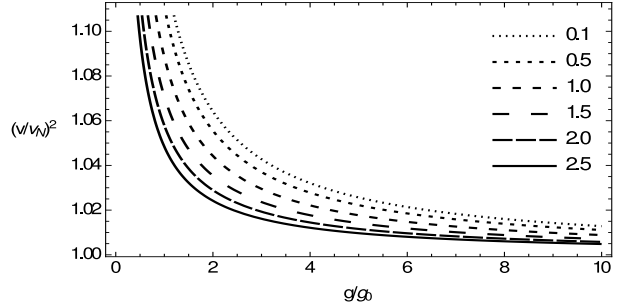


Fig. 6 Mass discrepancy $(\frac{v}{v_b})^2$ as a function of Newtonian gravitational field g for different values of $y = r/R_d = 0.1, 0.5, 1.0, 1.5, 2.0, 2.5$.

Eqs. (25) and (31) could explain another important feature of our model. From these two equations it is clear that all departure from pure Newtonian theory are included in the a_0 -dependent terms. Therefore, because both of the functions are solely dependent to baryonic matter, any feature in rotation curve data and dark matter profile should occur simultaneously. This is known as the Renzo's rule; i.e. "For any feature in the luminosity profile there is a corresponding feature in the rotation curve" (Sancisi 2004; McGaugh 2004). In fact any pure baryonic theory could explain this observational rule. It is important to note that all these results are achieved without assuming the dark matter hypothesis.

6 Data Analysis of 39 LSB galaxies

In this section we apply the model that we discussed above to a sample of 39 LSB galaxies. The names of the galaxies could be found in the first column of Table 3. The distance D , luminosity L_B and scale length R_d of each galaxy with the sources of the data are shown too. In this work, the presented distances of NED (NASA/IPAC Extragalactic Database), reported by Mannheim & O'Brien (2012), are used which are based on Cepheids, Tully-Fisher relation or redshift measurement. The estimated mass and mass to light ratio M/L , derived from the curve fitting, are reported in the table too. In this data analysis, the galactic mass of galaxies and the parameter c_1 are the free parameters of the fit. Following a discussion based on population synthesis model by Sanders (1996) and Mannheim & O'Brien (2012), we restricted the mass to light ratio to be larger than $0.2M_\odot/L_\odot$. Also we found that the best fitting

results are obtained when we restrict c_1 to be within the interval of $0.2 \times 0.065 \leq c_1 \leq 2.0 \times 0.065$ which seems to be reasonable due to our prior estimation of this parameter (Shenavar 2016 a). However, I should mention that the mean value that we found for c_1 in this data analysis appears to be about half of the predicted one $c_1 = 0.065$. In Shenavar (2016 a) we used last data points of galactic rotation curves and found that the mean value of c_1 in the case of LSB galaxies is generally smaller compared to that of HSB galaxies. The difference compared to $c_1 = 0.065$ was found about 7 % lower for LSBs while while 37 % higher for HSBs. Comparing to these prior results, the mean value of c_1 that we found here, i.e. $c_1 \approx 0.03$ needs more attention. The mean value is smaller, as we expected because we are dealing with LSBs; though it is half of the theoretical value. This might be due to our method of fitting or general uncertainties in the data. To find an accurate value for c_1 , we are urged to seek better fitting methods and more accurate data in future.

Another point is that no bulge is assumed in any of the cases. This presumption certainly affects the viability of the fitting in the inner parts of galaxies, though, it is clear that it should not strongly change the rotation velocity at outer sections of galaxies. The reason is that whatever new components we assume for galaxies, their contributions to the acceleration will converge to $2c_1a_0$ at large radii and thus it is independent of the shape of the new components. However, to obtain a better fitting result in inner parts, we intend to include the bulge contribution in future works.

Beside this, the vertical thickness of the disk is ignored too. Galactic disk scale lengths R_d are usually much larger than the galactic scale heights. It can be proved that the corrections due to thickness are only important in the inner parts of galaxies, and therefore have no significant effect on the outer parts which is dominant by the linear potential contribution (Mannheim 2006).

It is worthy to note that the derived mass in the present analysis encompasses all of the matter content of the galaxies including their gas and dust. Reading the amount of Hydrogen mass from literature, for example, one can multiply it by 4/3, inferred from big bang nucleosynthesis to include the amount of Helium, and derive the total mass of the gas. Usually a small fraction of galactic mass is due to the mass of primordial Hydrogen and Helium.

To evaluate the viability of any model, one prefers the rotation curve data to be extended at least ten times as the scale of the galaxies R_d . Unfortunately this is not the case for most of the cases and, as we see in Fig 8, there are some galaxies with data expanded just about

$2R_d$ or R_d or even less. According to the discussion that we had after Eq. (26), the rising, falling or constancy of the rotation curve will be clearly observed only after $r \approx 2R_d$. Therefore, it is not possible to decide about the accuracy of the model, with a high confident, unless we receive data at larger distances.

Another problem occurs when there are just a few number of data points and they are spread far from each other. For example check F563-V2 or ESO 4250180 in Fig. 7. Although in these cases the fit can explain the general behavior of the galactic rotation curve, we should not expect it to follow rotation curve in any single detail. The problem here lies within the mathematical method of fitting which is based on numerical optimization of functions using differential evolution. The more that we have data points, the more accurate the machine can solve the problem of minimizing and so we can find a better fitting.

Anyway, from Figs. 7 and 8 it is clear that, although we have not considered some of the details of galactic structures, like the presence of a bulge and the effect of disk thickness, our model can capture the general trend of the rotation curves of the present sample. In these figures, the contribution of the luminous Newtonian term alone is specified with large dashes while the contribution of the new term $2c_1a_0$ is shown with small dashes and the solid line shows the result of the nonlinear fitting of Eq. (25). The points with the error bars are the observational data.

However, we should point out that for three galaxies out of 39 - namely ESO 2060140, F730-V1 and UGC 11648 - the fitting curve lies above the data and so we observe some difficulties. For ESO 2060140 and UGC 11648, the curves show a magnitude roughly 25 % larger than the last data points while for the case of F730-V1 the situation is less serious. In the cases of F730-V1 and UGC 11648 we observed that if we reduce the scale of the galaxies by about 35 % we can capture the data much better, though this does not happen for ESO 2060140. See Fig. 9 for the rotation curves of these three galaxies assuming new galactic scale to be 0.65 times of that in Table 3. This might be a sign of a two-disk or bulge-disk scenario, because it shows that mass is concentrated in smaller radii, or even an overestimation of the galactic scale R_d .

We see clear flat rotation curves in the cases of UGC 11454, UGC 11748 and UGC 11616 while most of others seem to have rising rotation curves. Although as we argued before, for the galaxies with data spread bellow $r/(2R_d) \approx 1$ there isn't enough data to decide about the general trend of the rotation curve with confidence. In addition, we should mention that there is no falling rotation curve in this sample because there is no very

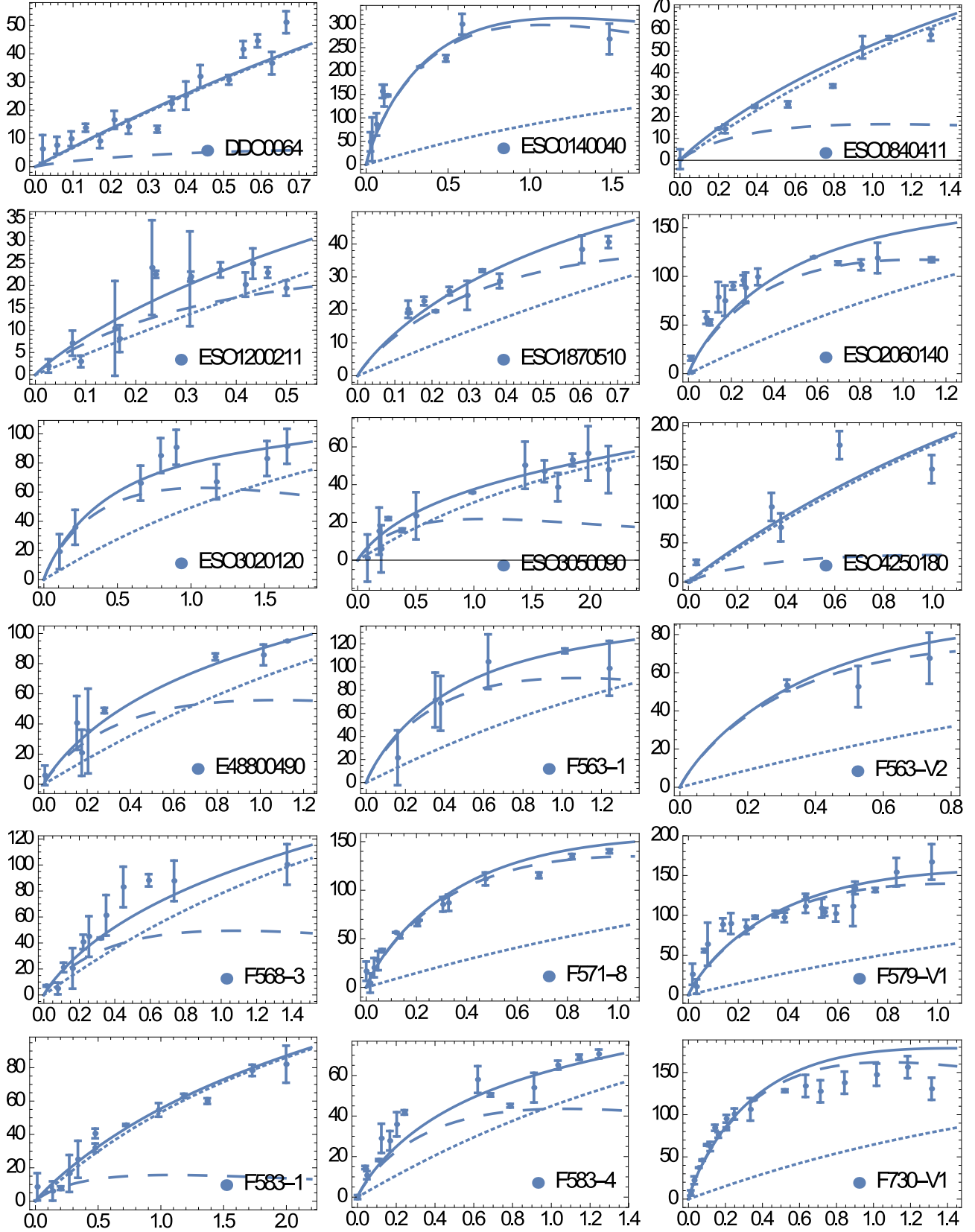


Fig. 7 Fitting of the galactic rotation curves v in km/s , with their error bars, as a function of the scaled radius $r/(2R_d)$ for a sample of 18 galaxies. The contribution due to the luminous Newtonian term alone is shown with large dashes while the contribution of the new term $2c_1a_0$ is shown with small dashes. Also, the solid line shows the result of the nonlinear fitting of Eq. (25) and the points with the error bars are from the observation.

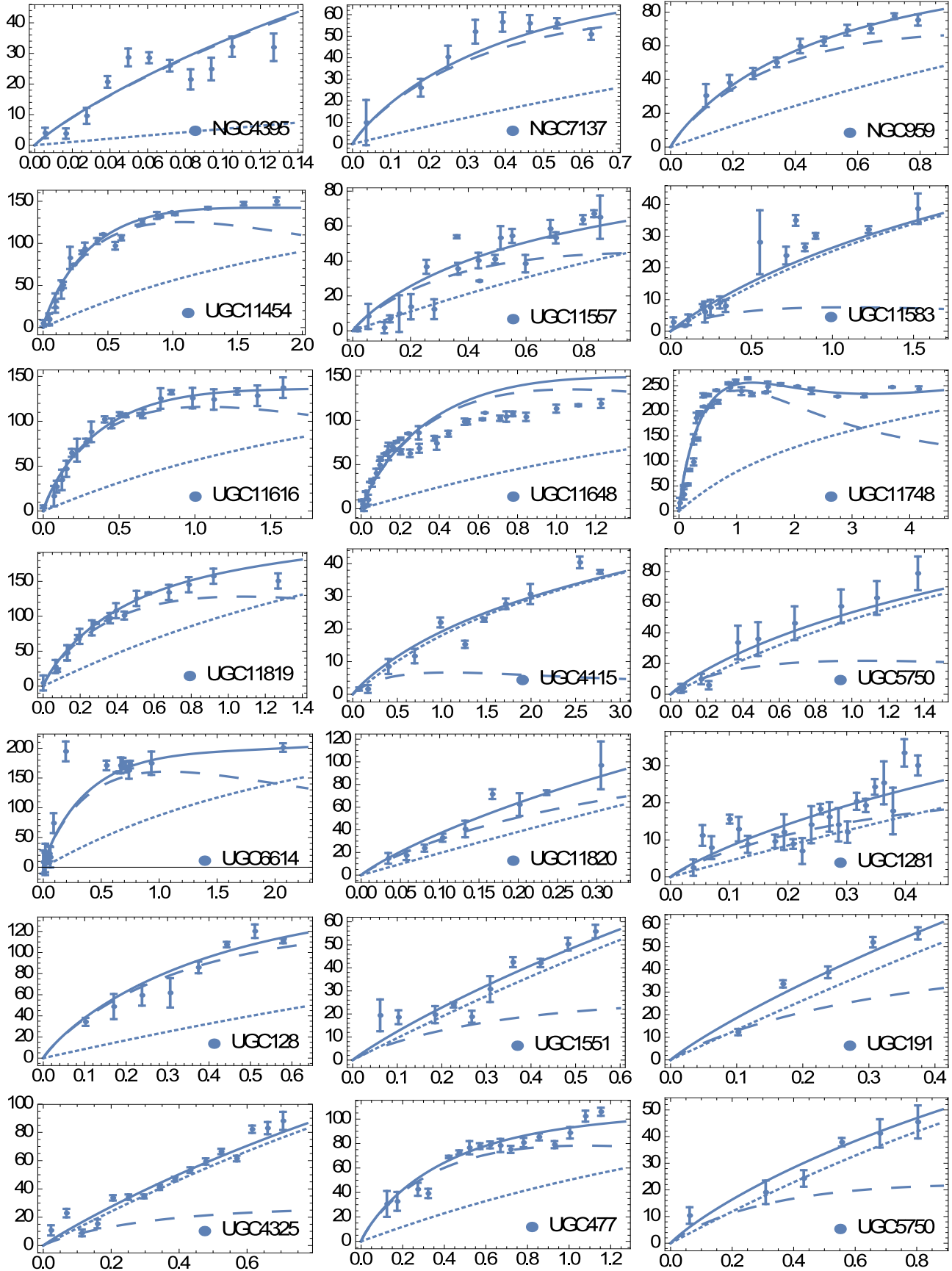


Fig. 8 Fitting of the galactic rotation curves v in km/s , with their error bars, as a function of the scaled radius $r/(2R_d)$ for a sample of 21 galaxies.

massive HSB galaxies. Including this class of galaxies - HSB galaxies - in rotation curve analysis remains as one of our main priorities for future works.

Population synthesis model (Sanders 1996) suggests an upper limit of mass to light ratio about $10M_{\odot}/L_{\text{odot}}$. From mass to light ratio column in Table 3 we see that there is only one galaxy, i.e. F571-8, for which we have found a very high M/L equal to about 31 though the fitting curve for this galaxy is quite good. For galaxies with small inclination angle one can argue that the total mass might be overestimated as Mannheim & O'Brien (2012) have argued about UGC 5999 with an inclination about 14° . However, the present case is nearly edge-on and thus the above argument is not applicable. On the hand there are uncertainties in photometric data because of the optical depth and projection effects. Our derived mass is about $5.89 \times 10^{10}M_{\odot}$ which is due to the galaxy's very high reported velocities. Therefore we have a clear problematic case here. Considering the uncertainty in photometric data in addition to the success of this model for the other galaxies it is possible that the luminosity might have been underestimated in this case.

It should be pointed out that to discuss the dynamics at cluster scales, or probably even huge galaxies with extended rotation curves, one needs to include the cosmological constant term Λ . In such cases a new term of the form $1/3\Lambda c^2 r$, r being the distance from the center of the galaxy, should be added to the equation of motion which has the effect of reducing rotation velocity. If we use the current value of cosmological constant $\Lambda \approx 10^{-52}m^{-2}$, it is possible to see that this term would be important beyond 200 kpc. Fig 10 explains this point for the case of ESO0140040. As you see, the rotation curve with the contribution of Λ , shown by solid line, will fall ultimately; otherwise, it will increase indefinitely as shown by small dashes. In the case of fourth-order conformal gravity too, there is a term similar to Λ which causes the ultimate fall off of rotation velocity (Mannheim & O'Brien 2012). Though, this happens at smaller radii, compared to our model, because Mannheim & O'Brien (2012) have assumed that the term responsible for the fall-off is of the order of $(1/100Mpc)^2 \approx 10^{-50}m^{-2}$. The role of cosmological constant should be studied more thoroughly in future works.

7 Conclusion

In this paper I started to investigate the consequences of a new equation of motion in weak field limit which is motivated by considering Neumann boundary condition

and spacetime measurement in an expanding universe. The new term in Eq. (1) is an intermediate effect between mere curved spacetime - which we use to describe strong fields around massive objects like black holes - and a flat FRW spacetime. We surveyed the consequences of the new term $2c_1 a_0 \hat{e}_r$ in solar and galactic scales and showed that it leads to some successful results.

In the case of clusters, external probes like lensing can be very helpful in providing a better understanding of the general features of these objects while interior probes, like X-ray kinematics and dynamics of single galaxies in a cluster, can equip us with more detailed knowledge. The same is true about satellite galaxies which can tell us more about the viability of the present model and specially the role of the Λ term.

Regarding the uncertainties in distances of galaxies which are not very high with our current methods - usually within a factor of two at most - and also the uncertainties in velocity data - which are at most about 20 % to 30 % - we see that the universality of acceleration at the last data point should be regarded as an important dynamical property of the galaxies. We discussed this matter in Shenavar (2016 a) and showed the near universality of the acceleration at the last data points for LSB and HSB galaxies. There we found that $c_{1LSB} = 0.060$ for LSB galaxies and $c_{1HSB} = 0.088$ for HSB galaxies. In the sample of HSB galaxies, there are a few galaxies with very high luminosities that show a value of Neumann constant about $10c_1$ or more. In these galaxies, the Newtonian term in the equation of motion is completely dominating the constant term $2c_1 a_0 \hat{e}_r$; thus we do not see a constant acceleration yet. However, excluding these data can help to find a better value of c_1 much closer to the value derived from Friedmann $c_1 = 0.065$.

One needs to appreciate the fact that galaxies have a variety of shapes and internal structures which, to achieve better rotation curve fittings, are needed to be included. Among these structures, the most important effect is due to the presence of bulge. The thickness of galaxies, in some cases, might be important too. We try to include these factors in future data analysis.

One might worry about the appearance of a new parameter c_1 in the present work, though, it should be noted that all models that try to solve the mass discrepancy problem, both DM models and modified gravities, have their new parameters. This is of course natural because, after all, we see a discrepancy between our Newtonian predictions and the observations which should be addressed by one or more new parameters. Of course, we prefer theories with less parameters. For example, if we accept the dark matter hypothesis, we

will need more parameters to go beyond the standard model of particle physics. For instance, supersymmetry could predict WIMPs, though this theory adds some new parameters to the standard model beside the main point that the existence of WIMPs is needed to be confirmed in detectors. In astrophysics of dark matter too, we need some new parameters to describe galactic/extragalactic effects of dark matter, two of which are mentioned in the NFW profile before. In this sense, the present model seems quite economical because it only possesses a single new parameter c_1 .

In MOND model too, we have a fundamental constant a_0 with various proposed interpolating functions μ . For now, it is inferred from MOND literature that the value $a_0 \approx 1.2 \times 10^{-10} \text{ms}^{-2}$ is accepted among them (Famaey & McGaugh 2012). This value is close to the value of our new term in the equation of motion $2c_1a_0 = 8.6 \times 10^{-11}$.

From a theoretical point of view, there still remain many other works to do. For example, according to Newtonian theory of gravity, galaxies and clusters are unstable without a dark matter halo (Ostriker & Peebles 1973; Mihos et al. 1997). This is in contrast with our repeated observations of galaxies and clusters which seem to be quite stable. However, numerical simulations have already proved that a linear potential is capable of providing stable disks without needing further matter or dark matter (Christodoulou 1991), we will check the stability - and other numerical features - of disk galaxies in a detailed numerical work in future.

Another important conspiracy is the mass estimation of galactic systems. For example, it is expected that for a cold disk of stars the total mass and virial velocity be related through the following equation: $v^3 \sim M$. Instead, according to successive observations, these two parameters are related through the famous Tully-Fisher law: $v^4 \sim M$. See Courteau (1997); McGaugh et al. (2000); Tully & Fisher (1977) for more details. Any successful modified dynamics/gravity should provide solid proof for this empirical fact and its zero point. Furthermore, the origin of exponential radial profiles in disk galaxies should be explained. These matters will be covered in another paper (Shenavar 2016 b).

Name	D (Mpc)	R_d (kpc)	Luminosity L_B ($10^{10} L_\odot$)	M_B ($10^{10} M_\odot$)	Derived M/L	c_1	RC Data Source
DDO0064	6.8	1.3	0.015	0.003	0.2	0.043	NMB NMBB
ESO0140040	217.8	10.1	7.169	54.086	7.544	0.013	MRB
ESO0840411	82.4	3.5	0.287	0.057	0.2	0.013	MRB
ESO1200211	15.2	2.	0.028	0.060	2.163	0.013	MRB
ESO1870510	16.8	2.1	0.054	0.177	3.287	0.013	MRB
ESO2060140	59.6	5.1	0.735	4.208	5.725	0.027	MRB
ESO3020120	70.9	3.4	0.717	0.809	1.128	0.013	MRB
ESO3050090	13.2	1.3	0.186	0.037	0.2	0.013	MRB
ESO4250180	88.3	7.3	2.6	0.52	0.2	0.076	MRB
E48800490	64.6	6.9	0.139	1.292	9.292	0.013	MRB
F563-1	46.8	2.9	0.14	1.426	10.184	0.029	MRB NMB NMBB
F563-V2	57.8	2.	0.266	0.639	2.403	0.013	MRB NMB NMBB
F568-3	80.	4.2	0.351	0.616	1.756	0.026	MRB NMB NMBB
F571-8	50.3	5.4	0.191	5.897	30.872	0.013	MRB
F579-V1	86.9	5.2	0.557	6.109	10.969	0.013	MRB
F583-1	32.4	1.6	0.064	0.024	0.370	0.032	MRB NMB NMBB
F583-4	50.8	2.8	0.096	0.319	3.325	0.013	MRB NMB NMBB
F730-V1	148.3	5.8	0.756	9.163	12.121	0.013	MRB
NGC4395	4.1	2.7	0.374	1.824	4.877	0.013	NMB NMBB
NGC7137	25.	1.7	0.959	0.349	0.364	0.013	NMB NMBB
NGC959	13.5	1.3	0.333	0.352	1.056	0.040	NMB NMBB
UGC11454	93.9	3.4	0.456	3.205	7.029	0.017	MRB
UGC11557	23.7	3.	1.806	0.361	0.2	0.013	MRB
UGC11583	7.1	0.7	0.012	0.002	0.2	0.016	MRB
UGC11616	74.9	3.1	2.159	2.512	1.163	0.018	MRB
UGC11648	49.	4.	4.073	4.387	1.077	0.013	MRB
UGC11748	75.3	2.6	23.93	9.042	0.378	0.043	MRB
UGC11819	61.5	4.7	2.155	4.638	2.152	0.040	MRB
UGC4115	5.5	0.3	0.004	0.0008	0.2	0.017	MRB BMR
UGC5750	56.1	3.3	0.472	0.094	0.2	0.013	MRB BMR
UGC6614	86.2	8.2	2.109	12.729	6.035	0.017	MRB BMR
UGC11820	17.1	3.6	0.169	2.108	12.474	0.13	NMB NMBB
UGC1281	5.1	1.6	0.017	0.0469	2.760	0.014	NMB NMBB
UGC128	64.6	6.9	0.597	5.703	9.553	0.014	NMB NMBB
UGC1551	35.6	4.2	0.78	0.156	0.2	0.027	BMR MRB
UGC191	15.9	1.7	0.129	0.170	1.31454	0.13	NMB NMBB
UGC4325	11.9	1.9	0.373	0.074	0.2	0.097	NMB NMBB
UGC477	35.8	3.5	0.871	1.289	1.480	0.013	NMB NMBB
UGC5750	56.1	3.3	0.472	0.094	0.2	0.014	NMB NMBB

Table 3 Properties of 39 LSB galaxies. Data of distance of galaxies D (Mpc), the scale length of galaxies R_d (kpc) and their luminosity L_B ($10^{10} L_\odot$) is derived from [Mannheim & O'Brien \(2012\)](#). The rotation curve data is extracted from [de Blok et al. \(2001\)](#) shown as BMR, [McGaugh \(2001\)](#) shown as MRB, [Naray et al. \(2008\)](#) shown as NMB and shown as [Naray et al. \(2008\)](#) NMBB. We have derived the mass M_B ($10^{10} M_\odot$) and mass to light ratio M/L .

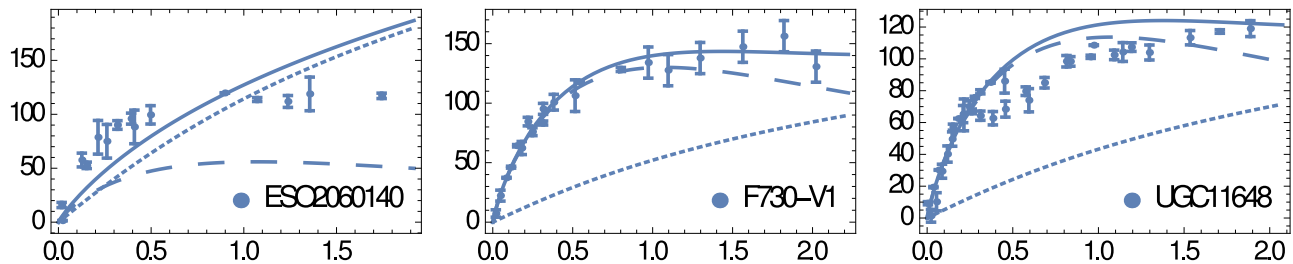


Fig. 9 Fitting of the galactic rotation curves v in km/s , with their error bars as a function of the scaled radius $r/(2R_d)$ for three galaxies which show some difficulties. Here it is assumed that the scale of the galaxies are 35 % smaller than the reported values in Table 3. This might be a sign of a two-disk or bulge-disk scenario. By this assumption F730-V1 and UGC 11648 show a better fit while ESO2060140 is still problematic.

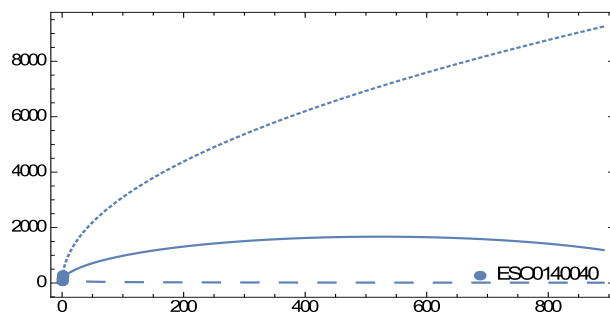


Fig. 10 Rotation curve v in km/s as a function of the scaled radius $r/(2R_d)$ for galaxy *ESO0140040*. The contribution due to the luminous Newtonian term alone is shown with large dashes while the contribution of the new term $2c_1a_0$ is shown with small dashes. The solid line shows the result of the nonlinear fitting of Eq. (25) plus the cosmological term $1/3\Lambda c^2 R_d^2 y^2$.

A Force Due to Some Geometrically Symmetrical Configurations and Their Virial Energy

In this section we study the force due to our modified equation of motion (1) using Eq. (21) for some useful configurations of matter. In addition, we derive the virial energy of these distributions from the next equation:

$$Vir = - \int d^3\vec{x} \rho(\vec{x}) \vec{x} \cdot \nabla \Phi \quad (\text{A1})$$

for future reference.

Spherical Shell : Consider a point particle with mass m located at a distance r from center of a shell with total mass of M and radius R . In addition, suppose that ρ and t are the density and thickness of this shell. Now, by using the new term in the force (21) , i.e. \vec{F}^{a_0} , which we introduced before we have:

$$\vec{F}^{a_0} = m \frac{2c_1 a_0}{M} \int \frac{\vec{x}' - \vec{x}}{|\vec{x}' - \vec{x}|} \rho(x') d^3 x' \quad (\text{A2})$$

it is possible to derive the inserted force on mass m outside of this shell as following:

$$F_{out}^{a_0} = \frac{2c_1 m a_0}{M} \frac{\pi t \rho R}{r^2} \int_{r-R}^{r+R} (r^2 - R^2 + x^2) dx \quad (\text{A3})$$

or $F_{out}^{a_0} = 2c_1 m a_0 (1 - \frac{R^2}{3r^2})$. Similarly, for a point particle inside the shell one has $F_{in}^{a_0} = \frac{4c_1 m a_0 r}{3R}$. The derivation is the same, but the lower limit of the integral is now $R - r$ instead of $r - R$. Note that these two forms of force coincide at $r = R$ and the net force vanishes at $r = 0$ as it is expected. Finally, it is possible to use (A1) and derive the virial energy due to the a_0 -dependent term for this configuration as $Vir_{a_0} = -2c_1 M R a_0$.

Isotropic Sphere : Consider a sphere with an isotropic mass distribution $\rho = \rho(x)$ and total mass M and radius R . Again, by using the term that is dependent to a_0 in Eq. (21) one may find the force F^{a_0} on a point particle m inside the sphere located at a distance r from the center of the sphere:

$$F^{a_0} = \frac{2c_1 m a_0}{M} \int \rho(x) \frac{(r - x \cos \theta) x^2 dx d\phi d \cos \theta}{\sqrt{r^2 + x^2 - 2rx \cos \theta}} \quad (\text{A4})$$

Here we have used the spherical symmetry of the system and neglected non-radial components of the force because of the symmetry. Starting with integration on θ , while the integral on ϕ is trivial, one can derive the force F^{a_0} exerted on a particle inside sphere:

$$F^{a_0} = \frac{4\pi c_1 m a_0}{M} \int_0^R \rho(x) x dx [r + x - |r - x| - \frac{r^3 + x^3 - (r^2 + rx + x^2)|r - x|}{3r^2}]$$

Homogeneous Sphere : For a homogeneous sphere, i.e. $\rho = \rho_0$, by careful evaluation of the last integral we find $F_{in}^{a_0} = 2c_1 m a_0 (r/R - 1/5(r/R)^3)$ for a particle inside the sphere and $F_{out}^{a_0} = 2c_1 m a_0 (1 - 1/5(R/r)^2)$ for a particle outside of the sphere. Again, the force vanishes at $r = 0$, approaches to $2c_1 m a_0$ at large radii and coincides at $r = R$. Now it is easy to find the virial energy of this sphere

$$Vir_{a_0} = \int_0^R \rho x \frac{F_{in}^{a_0}}{m} d^3 x \quad (\text{A5})$$

which we obtain $Vir_{a_0} = -36/35 M c_1 a_0 R$. For the case of Newtonian potential energy one obtains $Vir_N = -\frac{3GM^2}{5R}$

Exponential Sphere : Similarly, for an exponential isotropic spherical mass distribution, one could find the a_0 -dependent force from (A5). Setting $\rho = \rho_0 \exp(-r/R_d)$ and $R \rightarrow \infty$ into equation (A5) it is possible to find the following expression for the force:

$$F^{a_0} = 2c_1 m a_0 (1 - \frac{4}{u^2} + \exp(-u) \left[-\frac{1}{2} - \frac{u^2}{6} + 4 \frac{u+1}{u^2} \right]) \quad (\text{A6})$$

which we have used $u = r/R_d$ for more simplicity. Here R_d is the sphere scale length. To evaluate this equation one needs to use following integral:

$$\int x^m e^{cx} dx = \left(\frac{\partial}{\partial c}\right)^m \frac{e^{cx}}{c} = \frac{e^{cx}}{c} \sum_{k=0}^m (-1)^k \frac{D^{(k)} x^m}{c^k} \quad (\text{A7})$$

where $D^{(k)}$ is the k^{th} derivative operator. Please notify that this force vanishes at $r = 0$. To prove this one needs to use $-1/2 = \lim_{u \rightarrow 0} \frac{(u+1)\exp(-u)-1}{u^2}$. In addition, it is easy to check that at large radii one has $F^{a_0} = 2c_1 m a_0$. It is also possible to find this force in terms of modified Bessel functions. See [Mannheim \(2006\)](#) for more details. Although here we prefer to work with exponential function to manifestly explain the finite behavior of the force at very small and large radii. As the last step we calculate the virial energy by putting this force into equation (A5). Numerical evaluation of this integral is easy and we find $Vir_{a_0} = -(7/2)MR_d c_1 a_0$. By evaluating Newtonian virial energy for this mass distribution one could find $Vir_N = -\frac{5GM^2}{32R_d}$. Thus, the total virial energy of an exponential sphere becomes:

$$Vir = -\frac{5GM^2}{32R_d} - \frac{7}{2}c_1 a_0 MR_d \quad (\text{A8})$$

Exponential Disk : Now consider an exponential disk with an exponential surface mass density:

$$\Sigma(r) = \Sigma_0 \exp(-r/R_d) \quad (\text{A9})$$

in which R_d is the disk scale length. We already know that the Newtonian potential energy is $Vir_N = -11.63G\Sigma_0^2 R_d^3$. See [Binney & Tremaine \(2008\)](#). To derive the negative virial energy due to the constant acceleration, one should first derive the relevant force. For a mass distribution in cylindrical coordinate we use Eq. (22) to find the radial force which results in:

$$F^{a_0}(\varphi, r, z) = \frac{2c_1 m a_0}{M} \int_0^{2\pi} d\phi \int_0^\infty dZ \int_0^\infty R dR \rho(R, Z) \times \frac{r - R \cos(\varphi - \phi)}{(r^2 + R^2 - 2rR \cos(\varphi - \phi) + (Z - z)^2)^{1/2}} \quad (\text{A10})$$

If the mass distribution is cylindrically symmetric, like the situation that we have here, then the φ -component of force vanishes or equivalently we can consider $\varphi = 0$. Putting Bessel function expansion of Green function in cylindrical coordinate:

$$\frac{1}{(r^2 + R^2 - 2rR \cos(\varphi - \phi) + (Z - z)^2)^{1/2}} = \sum_{m=-\infty}^{+\infty} \int_0^\infty dk J_m(kr) J_m(kR) \exp[im(\phi - \varphi) - k |z - Z|] \quad (\text{A11})$$

into the prior equation and assuming that the mass distribution is very thin, i.e. $\rho(R, Z) = \Sigma(R)\delta(Z)$ we find that

$$F^{a_0}(r) = \frac{4c_1 \pi m a_0}{M} \int_0^\infty dk \int_0^\infty R dR \Sigma(R) (J_0(kr)J_0(kR) - R J_1(kr)J_1(kR)) \quad (\text{A12})$$

where all m-terms have vanished due to orthogonality conditions for periodic functions except $m = 0, 1$. Now we should use the following Bessel function integration:

$$\int_0^\infty R dR J_0(kR) \exp(-\alpha R) = \frac{\alpha}{(\alpha^2 + k^2)^{3/2}} \quad (\text{A13})$$

$$\int_0^\infty R^2 dR J_1(kR) \exp(-\alpha R) = \frac{3k\alpha}{(\alpha^2 + k^2)^{5/2}} \quad (\text{A14})$$

$$\int_0^\infty dk \frac{J_0(kr)}{(\alpha^2 + k^2)^{3/2}} = \frac{r}{2\alpha} \left(I_0\left(\frac{r\alpha}{2}\right) K_1\left(\frac{r\alpha}{2}\right) - I_1\left(\frac{r\alpha}{2}\right) K_0\left(\frac{r\alpha}{2}\right) \right) \quad (\text{A15})$$

to derive the final result for the a_0 -dependent term:

$$F^{a_0} = 4c_1 m a_0 y I_1(y) K_1(y) \quad (\text{A16})$$

where $y = r/2R_d$. In the last step we also have used some relations for differentiating Bessel functions such as $I'_0(z) = I_1(z)$, $I'_1(z) = I_0(z) - \frac{I_1}{z}$, $K'_0(z) = -K_1(z)$, $K'_1(z) = -K_0(z) - \frac{K_1}{z}$. This is a relatively tedious but straightforward calculation. It is also possible, as Mannheim has shown before [Mannheim \(2006\)](#), to start from the potential (22) and derive the same force. From the asymptotic expansion of modified Bessel functions:

$$K_\nu(z) \sim \sqrt{\frac{\pi e^{-2z}}{2z}} \left[1 + \frac{(4\nu^2 - 1^2)}{1!8z} + \frac{(4\nu^2 - 1^2)(4\nu^2 - 3^2)}{2!(8z)^2} + \dots \right] \quad (\text{A17})$$

$$I_\nu(z) \sim \sqrt{\frac{e^{2z}}{2\pi z}} \left[\left(1 - \frac{(4\nu^2 - 1^2)}{1!8z} + \frac{(4\nu^2 - 1^2)(4\nu^2 - 3^2)}{2!(8z)^2} + \dots \right) \right] \quad (\text{A18})$$

it is easy to prove that F^{a_0} vanishes at $r = 0$ and approaches to ma_0 in large radii.

Now we put this force into the definition of virial energy (A1) to obtain:

$$Vir_{a_0} = 64\pi c_1 a_0 \Sigma_0 R_d^3 \int_0^{+\infty} \exp(-2y) y^3 I_1(y) K_1(y) dy \quad (\text{A19})$$

It is easy to evaluate this last integral numerically. The answer is 0.092. Therefore, the virial energy of an exponential disk becomes:

$$Vir = -11.63/4\pi^2 \frac{GM^2}{R_d} - 2.94c_1 a_0 M R_d \quad (\text{A20})$$

The results for virial energy will be used in future.

Acknowledgements

I would like to thank the authors S. McGaugh, P. D. Mannheim, J. G. O'Brien W.J.G. de Blok, V. Rubin, K de Naray, A. Bosma, for providing their data freely. My special thank is to S. McGaugh who provided an easily available galactic database at <https://www.astro.umd.edu/ssm/data/>. Also, I thank Mohammad Moghadassi who helped me in some graphs. I acknowledge the anonymous reviewer whose comments helped to clarify the manuscript and especially improved comparisons with other theories. This research has made use of NASA's Astrophysics Data System.

References

- John D. Anderson, Philip A. Laing, Eunice L. Lau, Anthony S. Liu, Michael Martin Nieto, Slava G. Turyshev ;Phys.Rev.Lett. 81, 2858-2861 (1998)
- John D. Anderson, Philip A. Laing, Eunice L. Lau, Anthony S. Liu, Michael Martin Nieto, Slava G. Turyshev; Phys.Rev.D 65,082004,(2002)
- Anderson, J. D.; Turyshev, S.; Nieto, M. M. ; Bulletin of the American Astronomical Society, Vol. 34, p.1172 (2002)
- James J. Binney, Scot Tremaine, *Galactic Dynamics*, Princeton University Press, 2nd Edition, (2008)
- R. Bottema, J.L.G. Peetaa, B. Rothberg, and R.H. Sanders; Astron. Astroph. , 393, 453 -460, (2002)
- J. R. Brownstein, J. W. Moffat; ApJ, V. 636, Issue 2, pp. 721-74 (2006)
- W.J.G. de Blok, F. Walter, E. Brinks, C. Trachternach , Oh, S.-H. and R.C. Kennicutt Jr; Astronomical. J, 136, 26482719, (2008)
- W. J. G. de Blok, S. S. McGaugh, and V. C. Rubin, Astron. J. 122, 2396 (2001)
- S. Casertano; Mon. Not. R. Astron. Soc. 203 735 (1983)
- S. Casertano, and J. H. van Gorkom; Astronom. J. 101 (1991) 1231
- Sumanta Chakraborty, arXiv:1607.05986v1
- J. Charap and J. Nelson, J.Phys.A:Math.Gen. 16 (1983) 1661.
- Dimitris M. Christodoulou; ApJ, v.372, p.471 (1991)
- S. Courteau; Astronomical. J, 114, 2402, (1997)
- F. Donato, G. Gentile, P. Salucci, C. Frigerio Martins, M. I. Wilkinson, G. Gilmore, E. K. Grebel, A. Koch, R. Wyse; Mon. Not. Roy. Astron. Soc. 397, 11691176 (2009)
- Benoit Famaey and Stacy S. McGaugh, *Modified Newtonian Dynamics (MOND): Observational Phenomenology and Relativistic Extensions*, Living Rev. Relativity 15, (2012), 10 <http://www.livingreviews.org/lrr-2012-10>
- G. Gibbons and S. Hawking, Phys.Rev. D 15 (1977) 27522756
- Herbert Goldstein, Charles Poole, John Safko; *Classical Mechanics*, (Addison Wesley, 2002)
- Gron, O., Soleng, H. H. ApJ, v.456, p.445 (1996)
- Ray d'Inverno; *Introducing Einstein's Relativity Oxford University Press (1998)*
- Lorenzo Iorio; *M.N.R.A.S. Volume 419, Issue 3, pp. 2226-2232 (2012)*
- Chethan Krishnan, and Avinash Raju, arXiv:1605.01603v2
- J.C. Mihos, S.S. McGaugh, and W.J.G. de Blok; ApJ Lett., 477, L79, (1997)
- S.S. McGaugh, J.M. Schombert, G.D. Bothun and W.J.G. de Blok; ApJ, 533, L99L102, (2000)
- Stacy McGaugh, Federico Lelli, Jim Schombert, arXiv:1609.05917v1 (2016)
- McGaugh, Stacy S.; Rubin, Vera C.; de Blok, W. J. G; Astron. J. Volume 122, Issue 5, pp. 2381-2395 (2001)
- S.S. McGaugh, ApJ, 609, 652666, (2004)
- M. Milgrom, ApJ, 270, 365370, (1983)
- M. Milgrom, ApJ, 270, 371383, (1983)
- M. Milgrom, ApJ, 270, 384389, (1983)
- M. Milgrom, ApJ, vol. 287, (1984), p. 571-576
- M. Milgrom, ApJ, 338, 121127, (1989)
- M. Milgrom, Mon. Not. R. Astron. Soc., Volume 398, Issue 2, pp. 1023-1026. (2009)
- P. D. Mannheim, *Progress in Particle and Nuclear Physics, Volume 56, Issue 2, p. 340-445 (arXiv:astro-ph/0505266)*
- P. D. Mannheim, and D. Kazanas, ApJ, 342, 635 (1989)
- P. D. Mannheim, ApJ, 391, 429 (1992)
- P. D. Mannheim, ApJ, 419, 150 (1993). (hep-ph/9212304)
- P. D. Mannheim, November 1995. (astro-ph/9511045)
- Philip D. Mannheim, James G. O'Brien; Phys. Rev. D 85,124020 (2012) ,(arXiv:1011.3495)
- Kuzio de Naray, R., McGaugh, S.S., de Blok, W.J.G. , ApJ, 676, 920 (2008)
- Kuzio de Naray, R., McGaugh, S.S., de Blok, W.J.G., Bosma, A. , ApJS, 165, 461 (2006)
- Julio F. Navarro, Carlos S. Frenk, Simon D. M. White; ApJ, v.462, p.563 (1996)
- Julio F. Navarro, Carlos S. Frenk, Simon D. M. White; ApJ, v.490, p.49 (1997)
- R L Newburn, Jr, and D K Yeomans; *Annual Review of Earth and Planetary Sciences, Vol. 10: 297-326 (1982)*
- James G. O'Brien, Philip D. Mannheim; *MNRAS Volume 421, Issue 2, pp. 1273-1282 (2012)*
- Hans C. Ohanian, Remo Ruffini, *Gravitation and Spacetime Cambridge University Press; 3 edition (2013)*
- J.P. Ostriker, and P.J.E. Peebles; ApJ, 186, 467480, (1973)
- R. H. Sanders, ApJ, v.473, p.117 (1996)
- R. H. Sanders, M. A. W. Verheijen, ApJ v.503, p.97 (1998)
- R. H. Sanders, E. Noordermeer, Mon. Not. Roy. Astron. Soc., Volume 379, Issue 2, pp. 702-710 (2007)
- R.H. Sanders, *The Dark Matter Problem: A Historical Perspective, (Cambridge University Press, Cambridge; New York, 2010)*
- R. Sancisi, *The visible matter dark matter coupling, in Ryder, S., Pisano, D., Walker, M. and Freeman, K., eds., Dark Matter in Galaxies, IAU Symposium 220, 21-25 July, 2003, Sydney, Australia, IAU Symposium, 220, p. 233, (Astronomical Society of the Pacific, San Francisco, 2004)*
- J. Sultana, D. Kazanas, J. L. Said; Phys. Rev. D 86, 084008 (2012)
- Shenavar H., *Astrophysics and Space Science, V 361, article id.93, 20 pp (2016) doi: 10.1007/s10509-016-2676-5*
- Shenavar H., *In preparation.*
- R.B. Tully, and J.R. Fisher; Astron. Astroph, 54, 661673, (1977)
- John F. Wallin, David S. Dixon, Gary L. Page; ApJ.666:1296-1302 (2007)
- J. York, James W., Phys.Rev.Lett. 28 (1972) 10821085